Short-range correlation physics at low RG resolution

Anthony Tropiano[1], Scott Bogner[2], Dick Furnstahl[1]

[1]Ohio State University, [2]Michigan State University
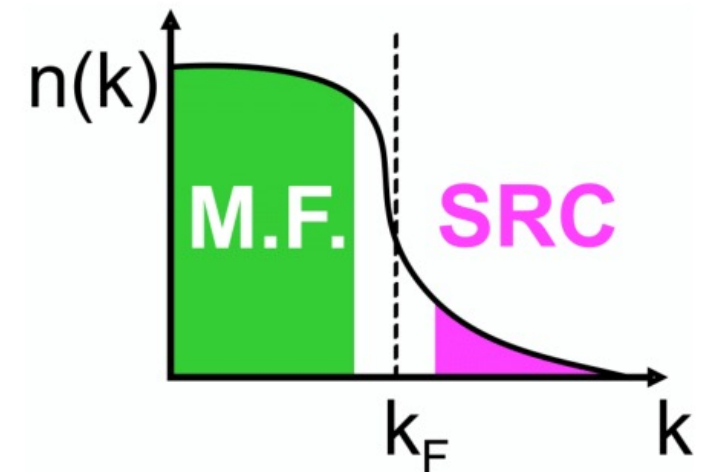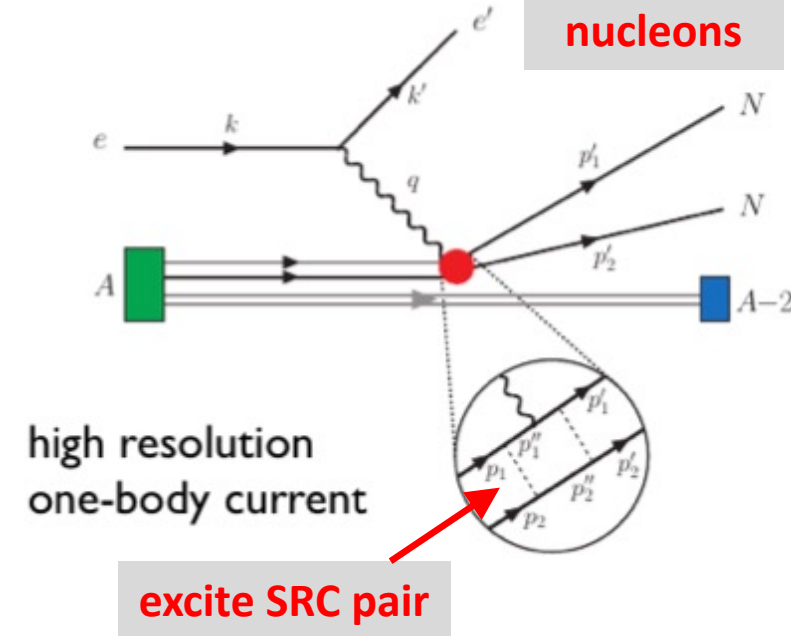
NUCLEI Annual Meeting

June 2, 2021

Motivation

- Recent experiments have been able to isolate processes where short-range correlation (SRC) physics is dominant and well accounted for by SRC phenomenology

- SRC physics at high RG resolution
  - SRC pairs are components in the nuclear wave function with relative momenta above the Fermi momentum

high resolution one-body current
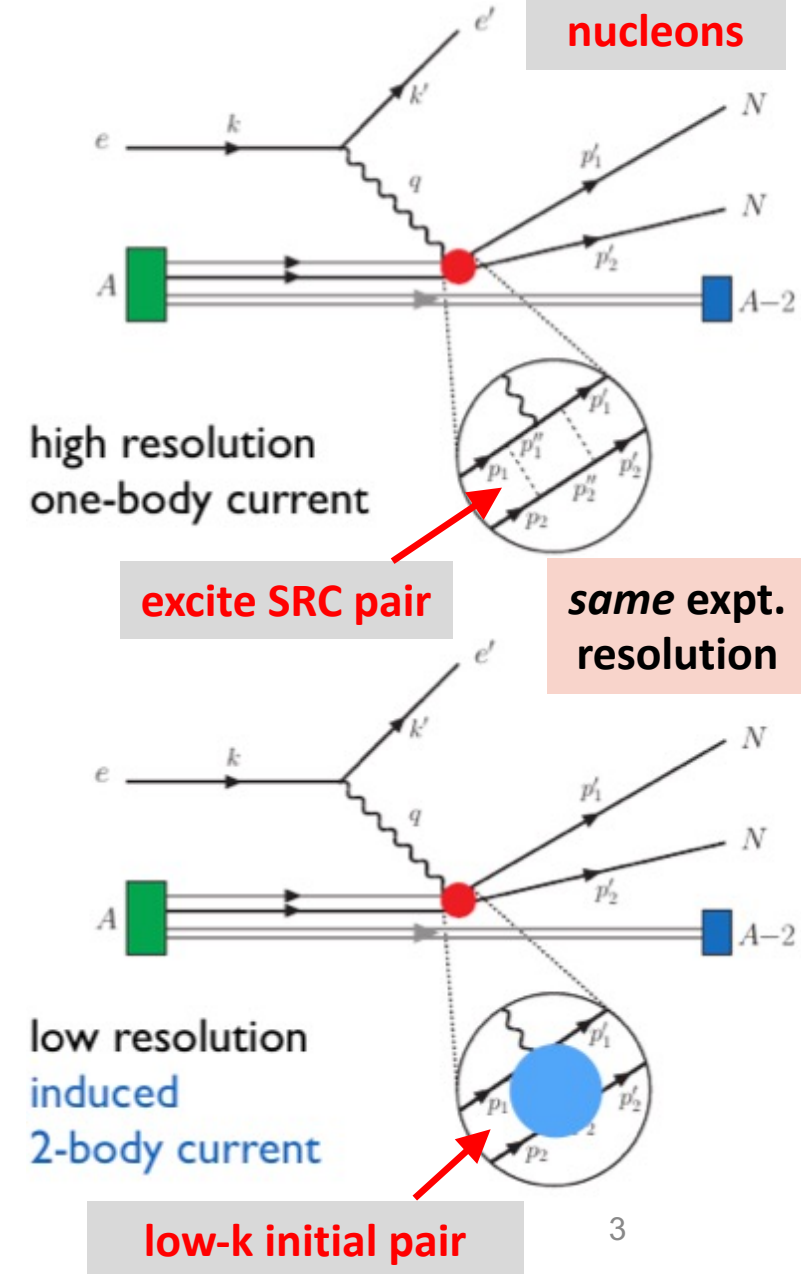
excite SRC pair

Motivation

- Recent experiments have been able to isolate processes where short-range correlation (SRC) physics is dominant and well accounted for by SRC phenomenology

- SRC physics at low RG resolution
  - The SRC *physics* is shifted into the reaction operators from the nuclear wave function (which becomes soft)
  - Operators do not become hard which simplifies calculations

knock-out 2 high-k nucleons

high resolution one-body current

excite SRC pair

same expt. resolution

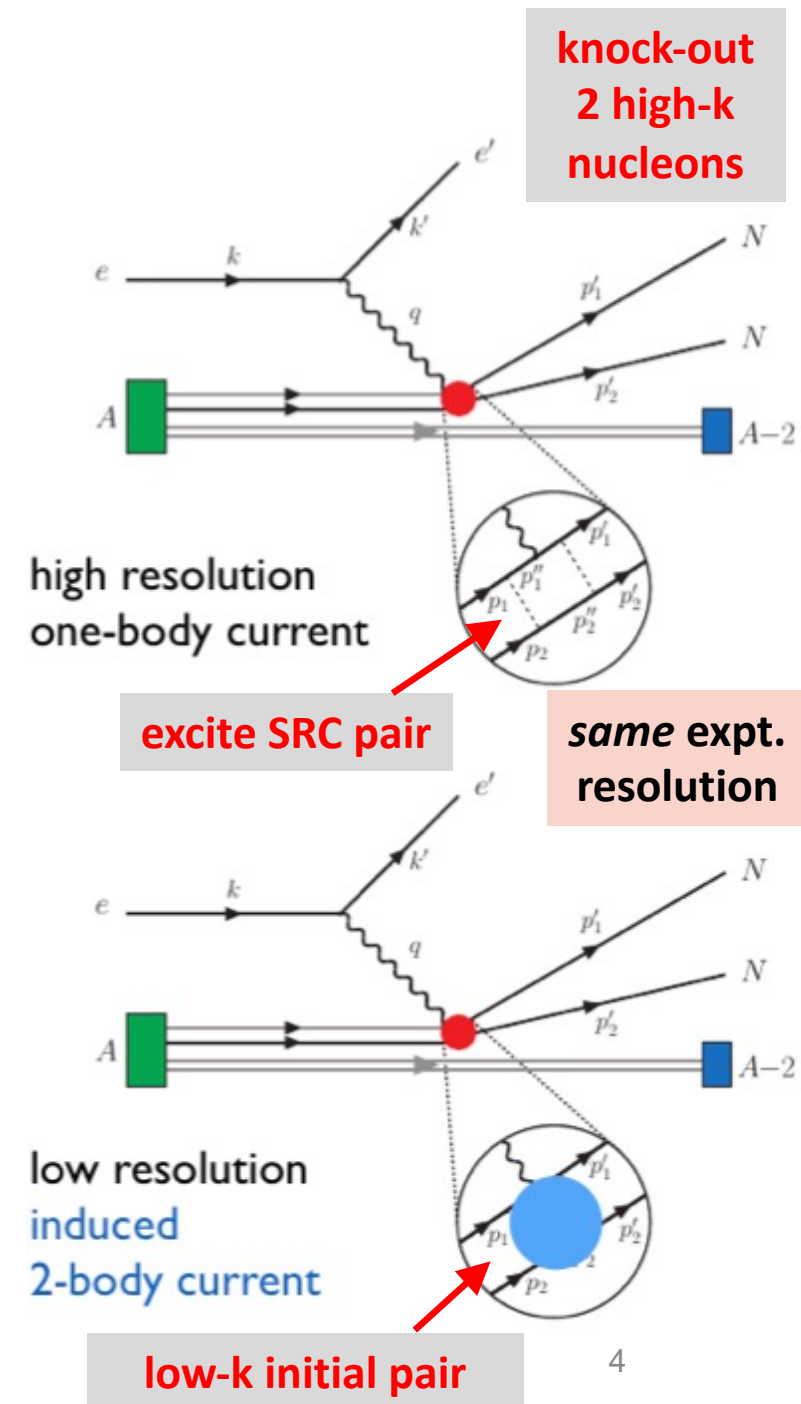low resolution induced 2-body current

low-k initial pair

Motivation

- Recent experiments have been able to isolate processes where short-range correlation (SRC) physics is dominant and well accounted for by SRC phenomenology

- SRC physics at low RG resolution
  - The SRC *physics* is shifted into the reaction operators from the nuclear wave function (which becomes soft)
  - Operators do not become hard which simplifies calculations

- Experimental resolution (set by momentum of probe) is the same in both pictures

- Same observables but different physical interpretation!

knock-out 2 high-k nucleons

high resolution one-body current

excite SRC pair

same expt. resolution

low resolution induced 2-body current

low-k initial pair

Similarity Renormalization Group (SRG)

- AV18 wave function has significant SRC

- What happens to the wave function at low RG resolution?

- Use SRG to unitarily evolve to low RG resolution where λ gives the decoupling scale
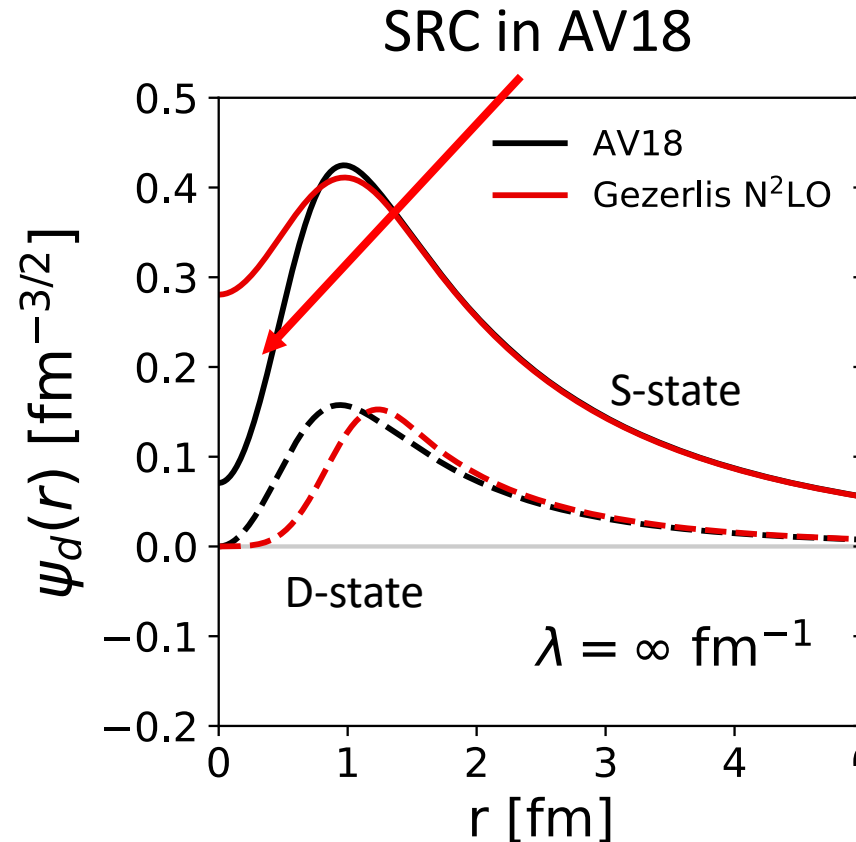

Fig. 2: SRG evolution of deuteron wave function in coordinate space for AV18 and Gezerlis N2LO[1].

[1]A. Gezerlis et al., Phys. Rev. C **90**, 054323 (2014)

Similarity Renormalization Group (SRG)

- SRC physics in AV18 is gone from wave function at low RG resolution

- Deuteron wave functions become soft and D-state probability goes down

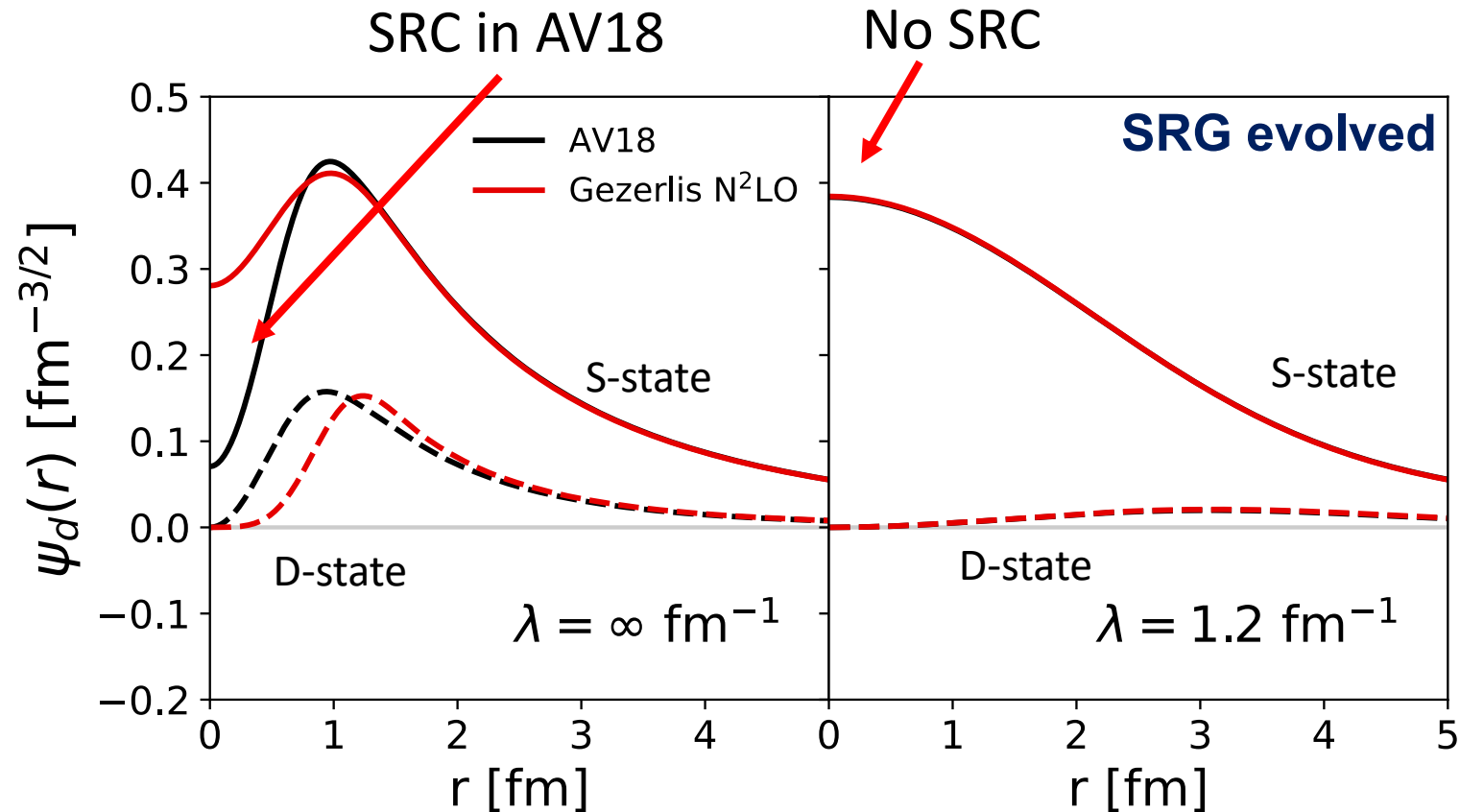- Observables such as asymptotic D-S ratio are the same

Fig. 2: SRG evolution of deuteron wave function in coordinate space for AV18 and Gezerlis N2LO[1].

[1]A. Gezerlis et al., Phys. Rev. C **90**, 054323 (2014)

Momentum distributions at low RG resolution

- Soft wave functions at low RG resolution
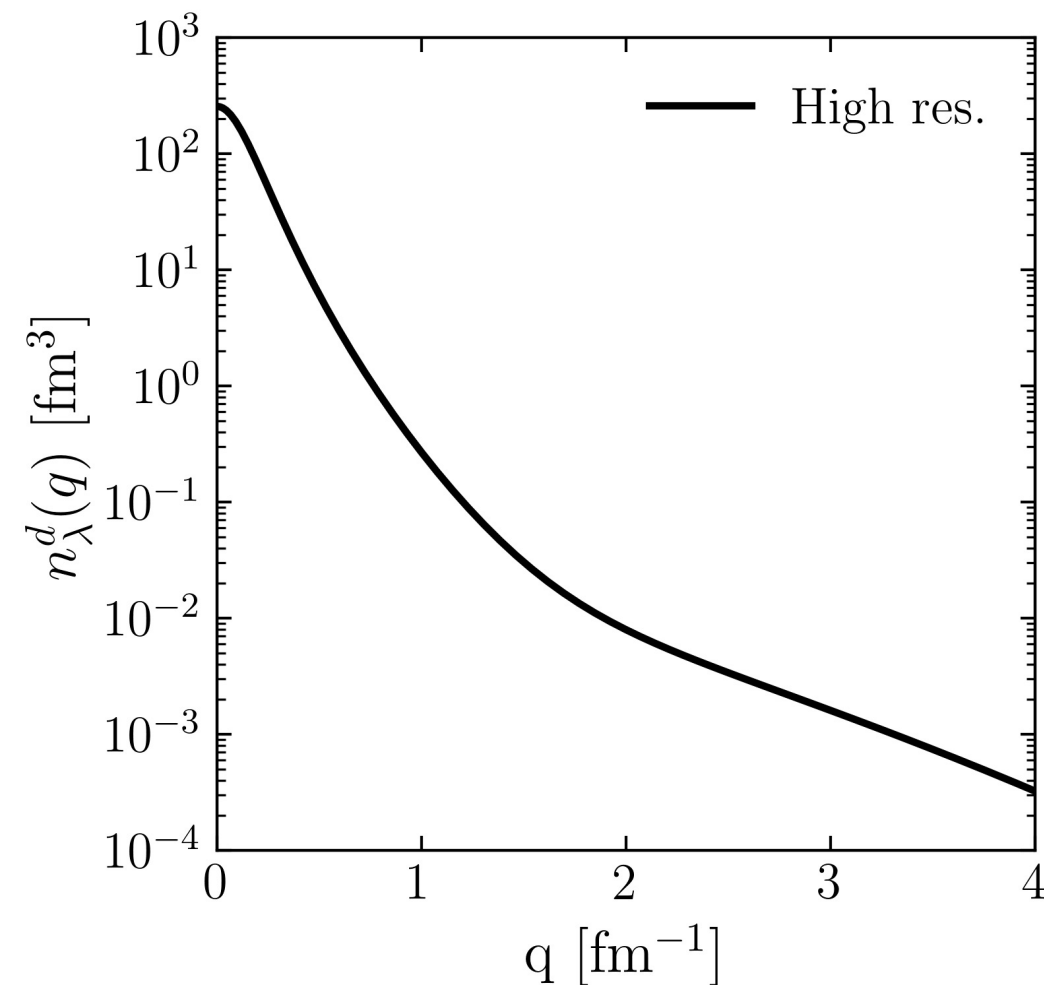 - Where does the SRC physics go?

Momentum distributions at low RG resolution

- Soft wave functions at low RG resolution
  - Where does the SRC physics go?

- SRC physics shifts to the operators $\langle \psi_f^{hi} | U_\lambda^\dagger U_\lambda O^{hi} U_\lambda^\dagger U_\lambda | \psi_i^{hi} \rangle$

- Apply SRG transformations to momentum distribution operator

$$n^{hi}(\boldsymbol{q}) = a_{\boldsymbol{q}}^\dagger a_{\boldsymbol{q}}$$

$$U_\lambda = 1 + \frac{1}{4} \sum_{\boldsymbol{K},\boldsymbol{k},\boldsymbol{k'}} \delta U_\lambda^{(2)}(\boldsymbol{k}, \boldsymbol{k'}) a_{\frac{K}{2}+\boldsymbol{k}}^\dagger a_{\frac{K}{2}-\boldsymbol{k}}^\dagger a_{\frac{K}{2}-\boldsymbol{k'}} a_{\frac{K}{2}+\boldsymbol{k'}} + \cdots$$

Momentum distributions at low RG resolution

Fig. 3: Contributions to deuteron momentum distribution with AV18 and $\lambda = 1.35$ fm^{-1}.

- Deuteron example

$$n^{lo}(\boldsymbol{q}) = (1 + \delta U) a_{\boldsymbol{q}}^{\dagger} a_{\boldsymbol{q}} (1 + \delta U^{\dagger})$$

$$\langle \psi_d^{hi} | a_{\boldsymbol{q}}^{\dagger} a_{\boldsymbol{q}} | \psi_d^{hi} \rangle$$

Momentum distributions at low RG resolution

Fig. 3: Contributions to deuteron momentum distribution with AV18 and $\lambda = 1.35$ fm^{-1}.

- Deuteron example

$$n^{lo}(\boldsymbol{q}) = (1 + \delta U)a_{\boldsymbol{q}}^{\dagger}a_{\boldsymbol{q}}(1 + \delta U^{\dagger})$$

$$\langle \psi_d^{hi} | a_{\boldsymbol{q}}^{\dagger}a_{\boldsymbol{q}} | \psi_d^{hi} \rangle$$
$$\langle \psi_d^{lo} | a_{\boldsymbol{q}}^{\dagger}a_{\boldsymbol{q}} | \psi_d^{lo} \rangle$$

Momentum distributions at low RG resolution

Fig. 3: Contributions to deuteron momentum distribution with AV18 and $\lambda = 1.35$ fm^{-1}.

- Deuteron example

$$n^{lo}(\boldsymbol{q}) = (1 + \delta U)a_{\boldsymbol{q}}^{\dagger}a_{\boldsymbol{q}}(1 + \delta U^{\dagger})$$

$$\langle\psi_d^{hi}|a_{\boldsymbol{q}}^{\dagger}a_{\boldsymbol{q}}|\psi_d^{hi}\rangle$$

$$\langle\psi_d^{lo}|a_{\boldsymbol{q}}^{\dagger}a_{\boldsymbol{q}}|\psi_d^{lo}\rangle$$

$$\langle\psi_d^{lo}|\delta U a_{\boldsymbol{q}}^{\dagger}a_{\boldsymbol{q}} + a_{\boldsymbol{q}}^{\dagger}a_{\boldsymbol{q}}\delta U^{\dagger}|\psi_d^{lo}\rangle$$

Momentum distributions at low RG resolution

Fig. 3: Contributions to deuteron momentum distribution with AV18 and $\lambda = 1.35$ fm^{-1}.

- Deuteron example

$$n^{lo}(\boldsymbol{q}) = (1 + \delta U) a_{\boldsymbol{q}}^{\dagger} a_{\boldsymbol{q}} (1 + \delta U^{\dagger})$$

$$\langle \psi_d^{hi} | a_{\boldsymbol{q}}^{\dagger} a_{\boldsymbol{q}} | \psi_d^{hi} \rangle$$

$$\langle \psi_d^{lo} | a_{\boldsymbol{q}}^{\dagger} a_{\boldsymbol{q}} | \psi_d^{lo} \rangle$$

$$\langle \psi_d^{lo} | \delta U a_{\boldsymbol{q}}^{\dagger} a_{\boldsymbol{q}} + a_{\boldsymbol{q}}^{\dagger} a_{\boldsymbol{q}} \delta U^{\dagger} | \psi_d^{lo} \rangle$$

$$\langle \psi_d^{lo} | \delta U a_{\boldsymbol{q}}^{\dagger} a_{\boldsymbol{q}} \delta U^{\dagger} | \psi_d^{lo} \rangle$$

Momentum distributions at low RG resolution

Fig. 3: Contributions to deuteron momentum distribution with AV18 and $\lambda = 1.35$ fm^{-1}.

- For high-q, the $\delta U_\lambda \delta U_\lambda^\dagger$ 2-body term dominates

$$\approx \sum_{\mathbf{K},\mathbf{k},\mathbf{k'}} \delta U_\lambda(\mathbf{k},\mathbf{q}) \delta U_\lambda^\dagger(\mathbf{q},\mathbf{k'}) a_{\frac{\mathbf{K}}{2}+\mathbf{k}}^\dagger a_{\frac{\mathbf{K}}{2}-\mathbf{k}}^\dagger a_{\frac{\mathbf{K}}{2}-\mathbf{k'}} a_{\frac{\mathbf{K}}{2}+\mathbf{k'}}$$

Momentum distributions at low RG resolution

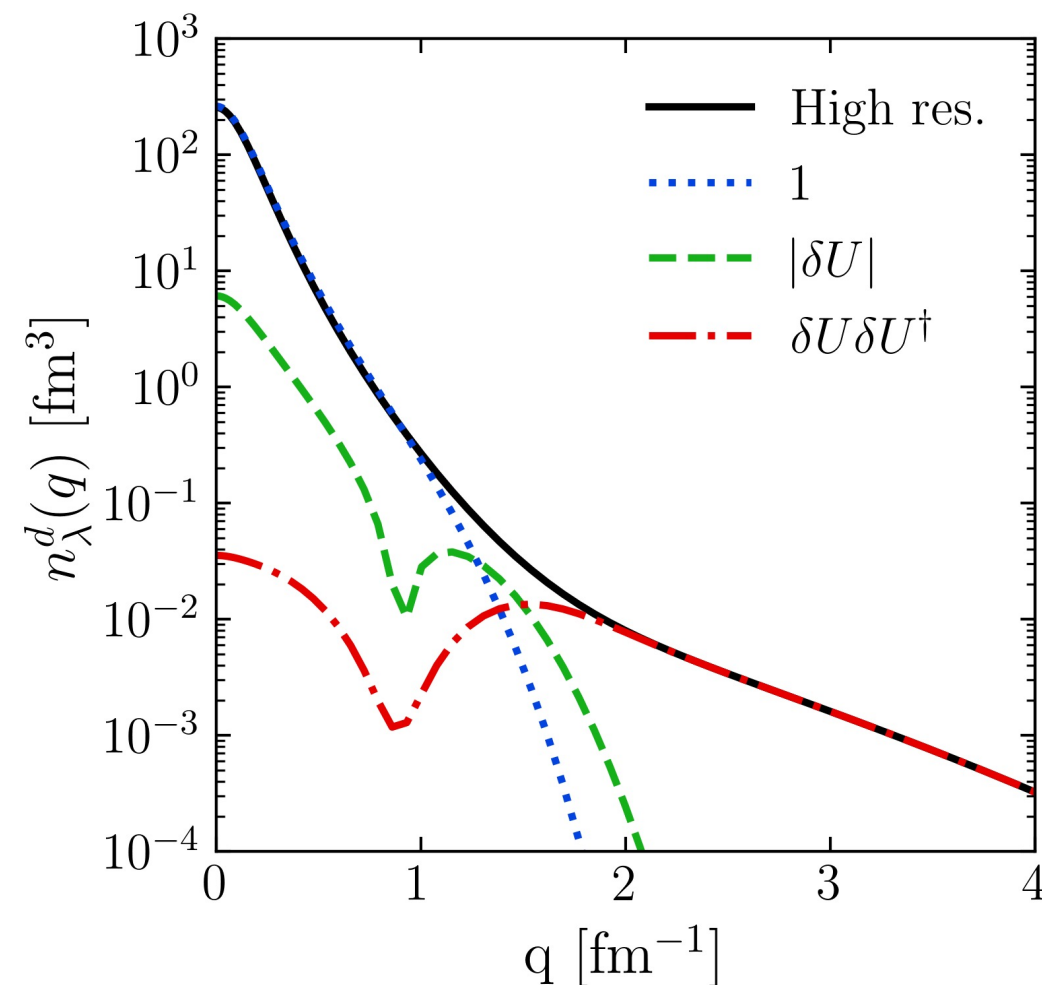**Fig. 3**: Contributions to deuteron momentum distribution with AV18 and $\lambda = 1.35$ fm^{-1}.

- For high-q, the $\delta U_\lambda \delta U_\lambda^\dagger$ 2-body term dominates

$$\approx \sum_{K,k,k'} \delta U_\lambda(k,q) \delta U_\lambda^\dagger(q,k') a_{\frac{K}{2}+k}^\dagger a_{\frac{K}{2}-k}^\dagger a_{\frac{K}{2}-k'} a_{\frac{K}{2}+k'}$$

$\downarrow$

Factorization: $\delta U_\lambda(k,q) \approx F_\lambda^{lo}(k) F_\lambda^{hi}(q)$

$\downarrow$

$$\approx \left| F_\lambda^{hi}(q) \right|^2 \sum_{K,k,k'}^\lambda F_\lambda^{lo}(k) F_\lambda^{lo}(k') a_{\frac{K}{2}+k}^\dagger a_{\frac{K}{2}-k}^\dagger a_{\frac{K}{2}-k'} a_{\frac{K}{2}+k'}$$

Momentum distributions at low RG resolution

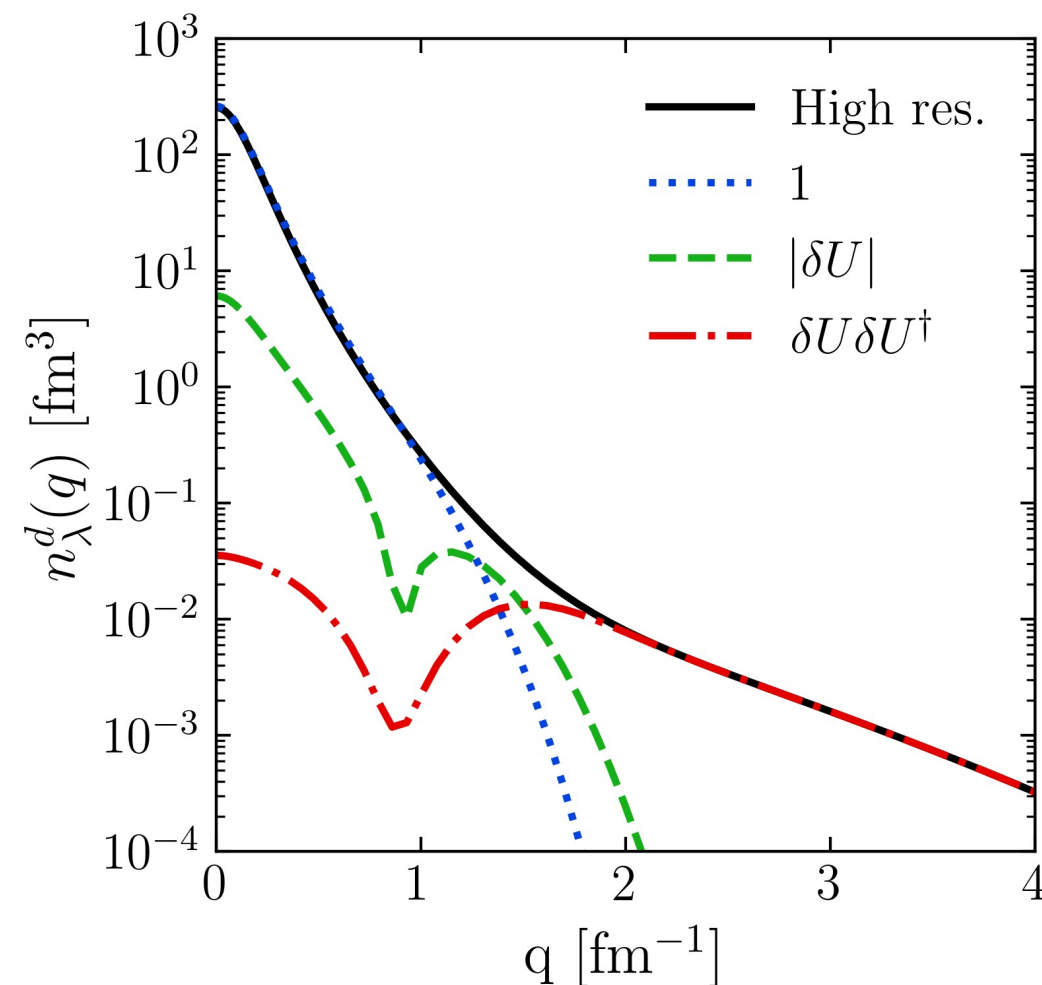**Fig. 3**: Contributions to deuteron momentum distribution with AV18 and $\lambda = 1.35$ fm^{-1}.

- For high-q, the $\delta U_\lambda \delta U_\lambda^\dagger$ 2-body term dominates

$$\approx \sum \delta U_\lambda(\boldsymbol{k}, \boldsymbol{q}) \delta U_\lambda^\dagger(\boldsymbol{q}, \boldsymbol{k}') a_{\frac{K}{2}+k}^\dagger a_{\frac{K}{2}-k}^\dagger a_{\frac{K}{2}-k'} a_{\frac{K}{2}+k'}$$

Apply this strategy to nuclear
momentum distributions using
local density approximation (LDA)!

$$F_\lambda^{hi}(\boldsymbol{q})$$

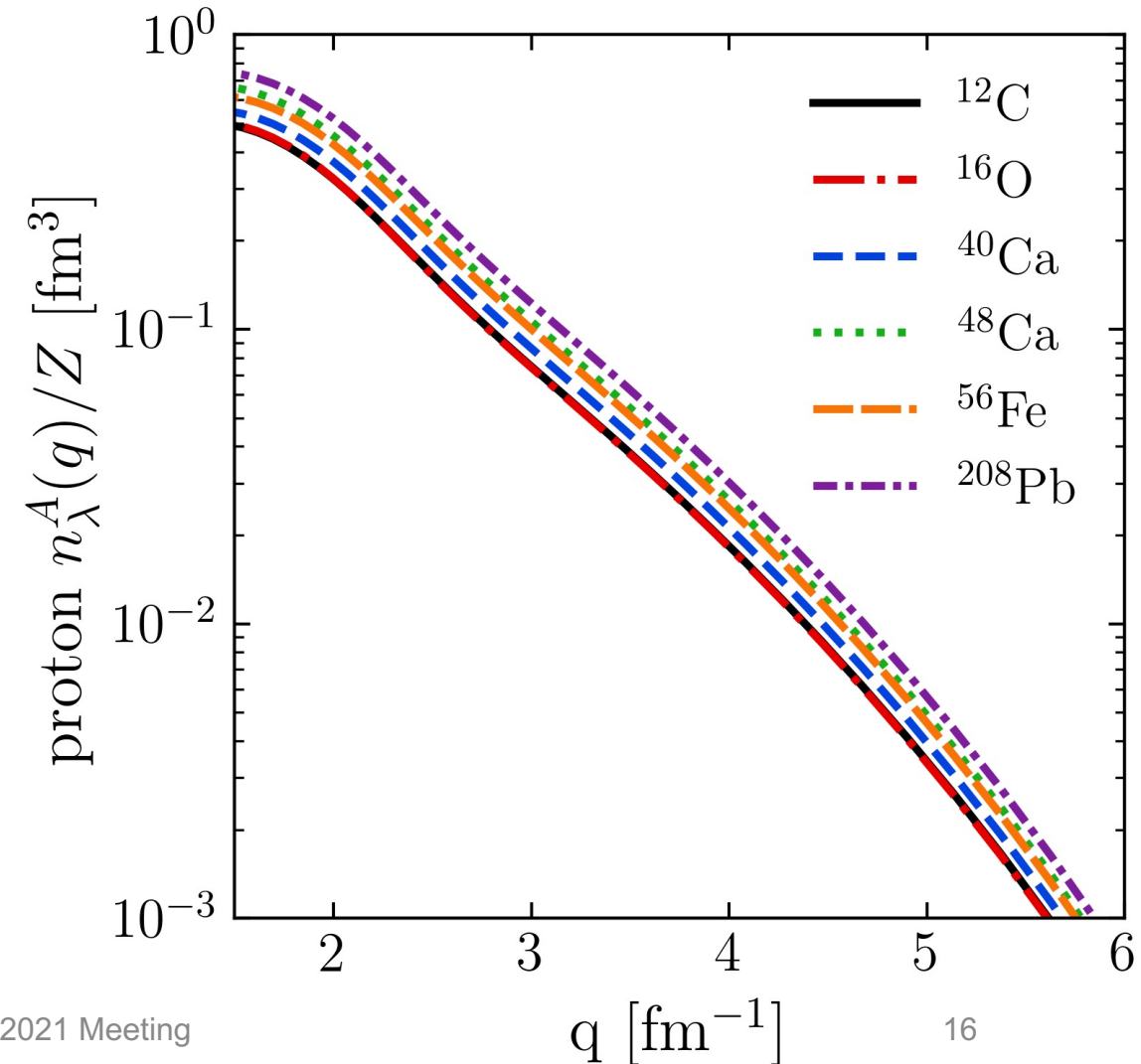$$\approx \left|F_\lambda^{lo}(\boldsymbol{q})\right|^2 \sum_{K,k,k'} F_\lambda^{lo}(\boldsymbol{k}) F_\lambda^{lo}(\boldsymbol{k}') a_{\frac{K}{2}+k}^\dagger a_{\frac{K}{2}-k}^\dagger a_{\frac{K}{2}-k'} a_{\frac{K}{2}+k'}$$

LDA results

- ## Universality

  - High-q tail collapses to universal function $\approx \left| F_\lambda^{hi}(\boldsymbol{q}) \right|^2$ fixed by 2-body
  - Results are insensitive to type of density

Fig. 4: Proton momentum distribution under LDA with AV18, $\lambda = 1.35$ fm^{-1}, and densities from Skyrme EDF SLy4 using the HFBRAD code[1].

[1]K. Bennaceur et al., Comput. Phys. Commun. **168**, 96 (2005)

LDA results

- Low RG resolution calculations reproduce momentum distributions of AV18 data[1] (high RG resolution calculation)

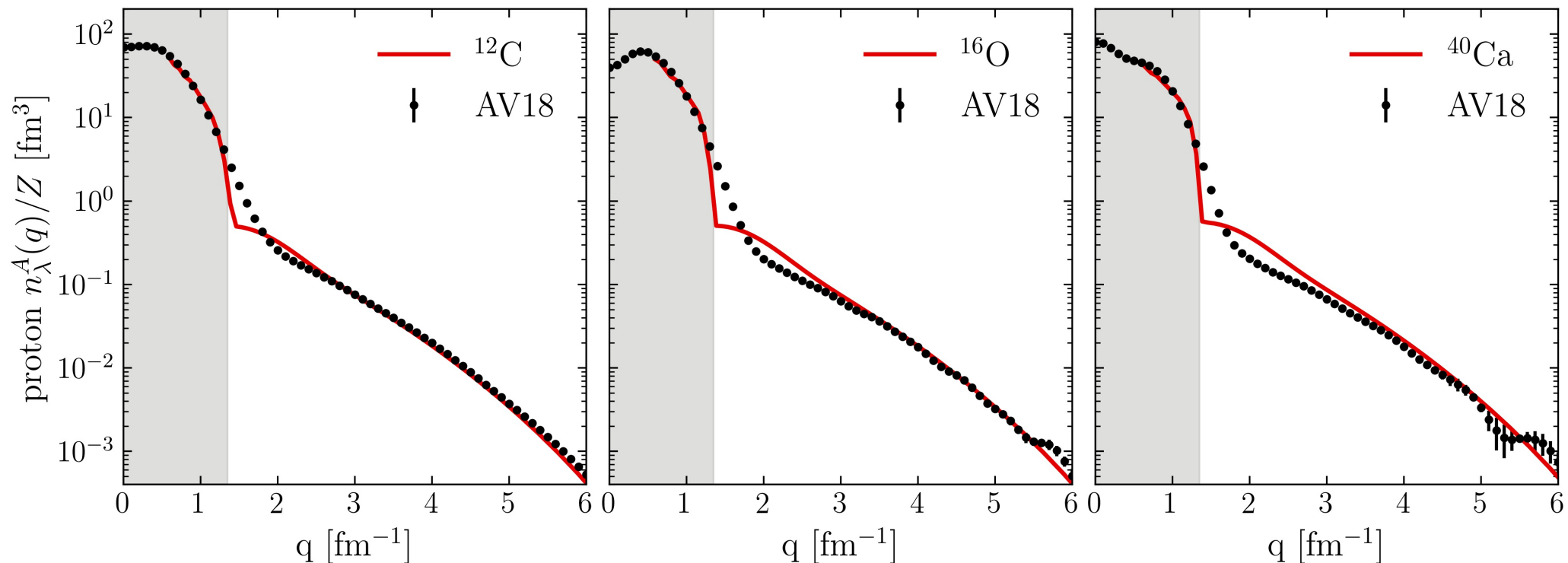- Low RG works well with simple approximations and is systematically improvable

Fig. 5: Proton momentum distributions for ^{12}C, ^{16}O, and ^{40}Ca under LDA with AV18 and $\lambda = 1.35$ fm^{-1}.

LDA results

np includes $^1S_0$ and $^3S_1$-$^3D_1$

Scalar limit

- At high RG resolution, the tensor force and the repulsive core of the NN interaction kicks nucleon pairs into SRCs

- np dominates because the tensor force requires spin triplet pairs (pp are spin singlets)

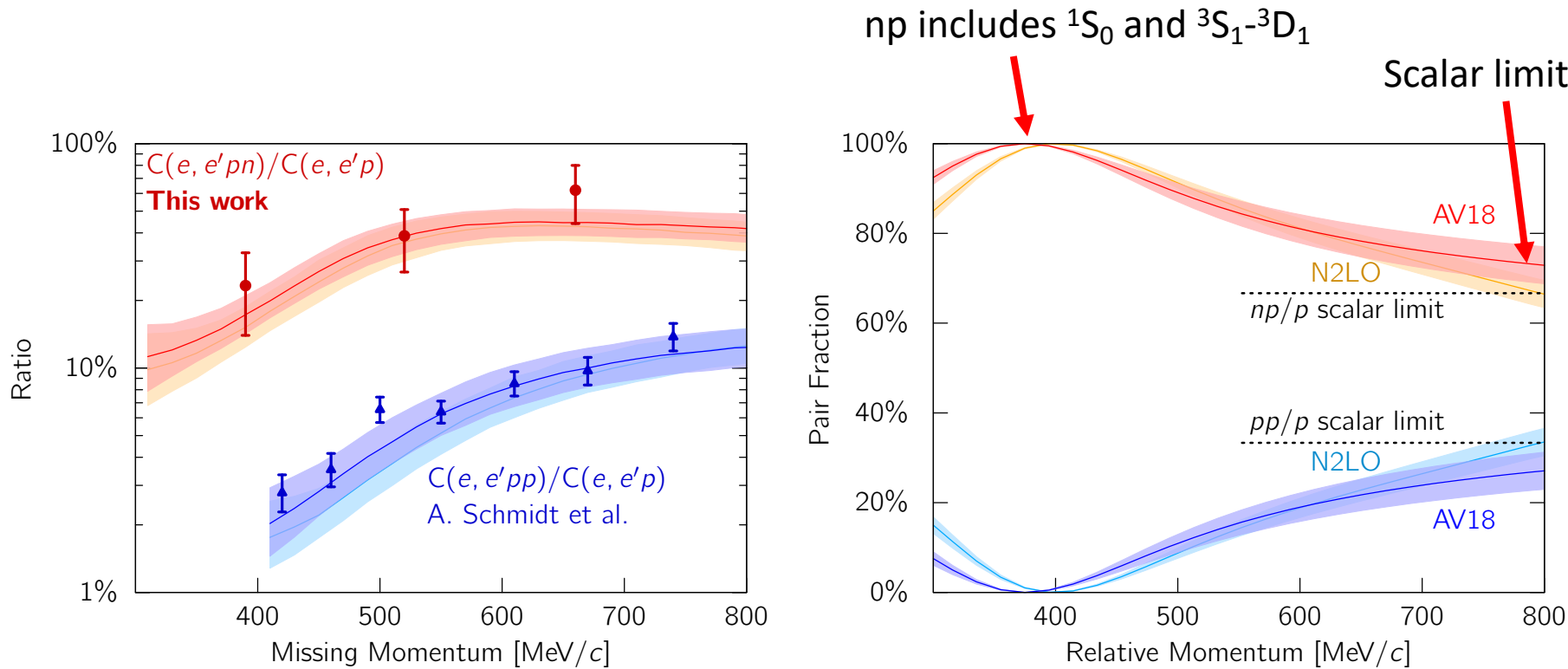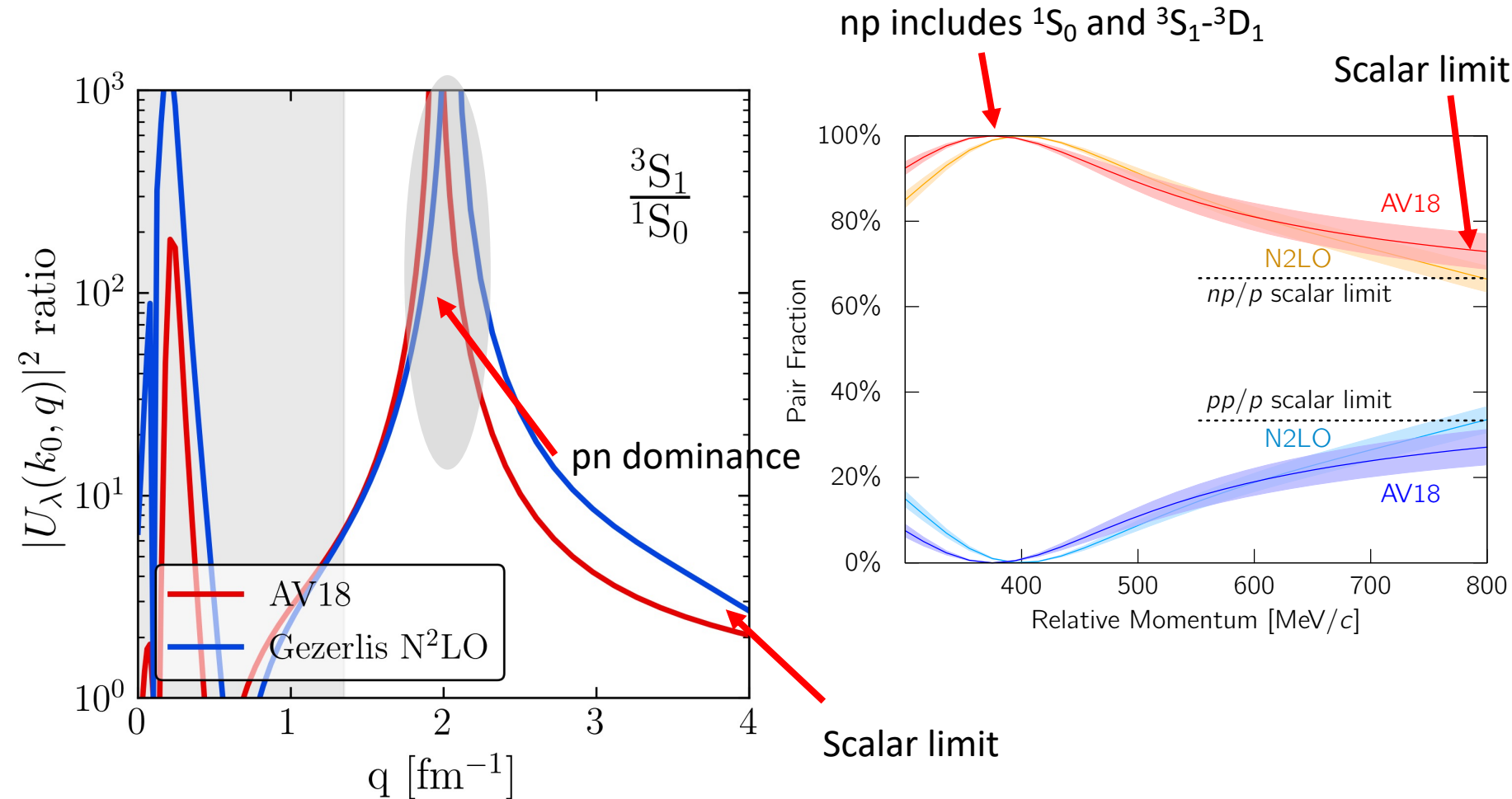- Do we describe this physics at low RG resolution?

Fig. 6: (a) Ratio of two-nucleon to single-nucleon electron-scattering cross sections for carbon as a function of missing momentum. (b) Fraction of np to p and pp to p pairs versus the relative momentum. Figure from CLAS collaboration publication[1].

[1]I. Korover et al. (CLAS), arXiv:2004.07304 (2014)

LDA results

np includes $^1S_0$ and $^3S_1$-$^3D_1$

Scalar limit

Scalar limit

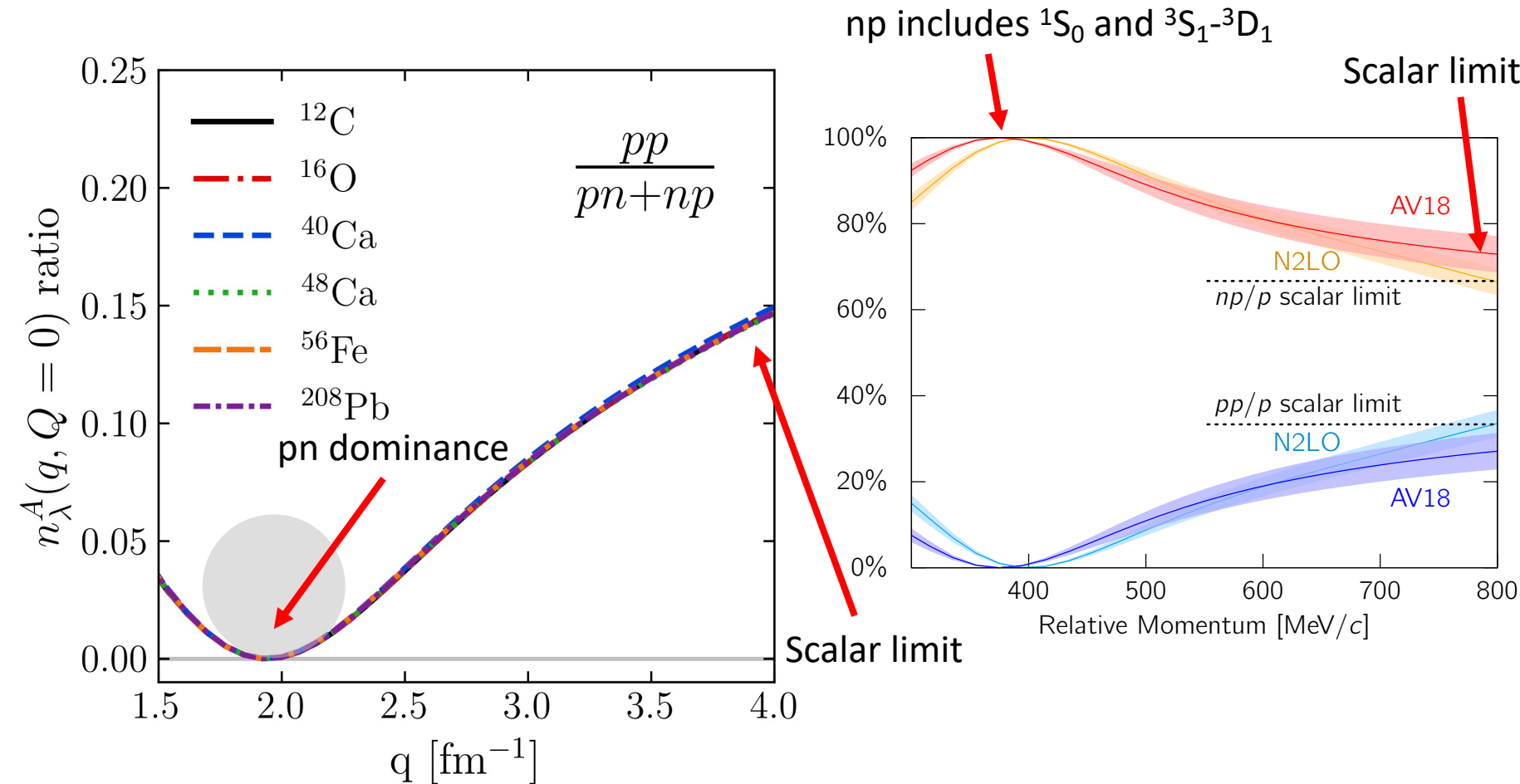Fig. 7: $^3S_1$ to $^1S_0$ ratio of SRG-evolved momentum projection operators $a_q^\dagger a_q$.

- At **low RG resolution**, SRCs are suppressed in the wave function
- Consider the ratio of $^3S_1$-$^3D_1$ to $^1S_0$ evolved momentum projection operator $a_q^\dagger a_q$
- **This physics is established in the 2-body system!**
- **Can apply to any nucleus!**

LDA results

np includes $^1S_0$ and $^3S_1$-$^3D_1$

Scalar limit

pn dominance

Scalar limit

$$\frac{pp}{pn+np}$$

Legend:
- ^{12}C
- ^{16}O
- ^{40}Ca
- ^{48}Ca
- ^{56}Fe
- ^{208}Pb

$n_\lambda^A(q, Q=0)$ ratio

q [fm^{-1}]

AV18
N2LO
np/p scalar limit
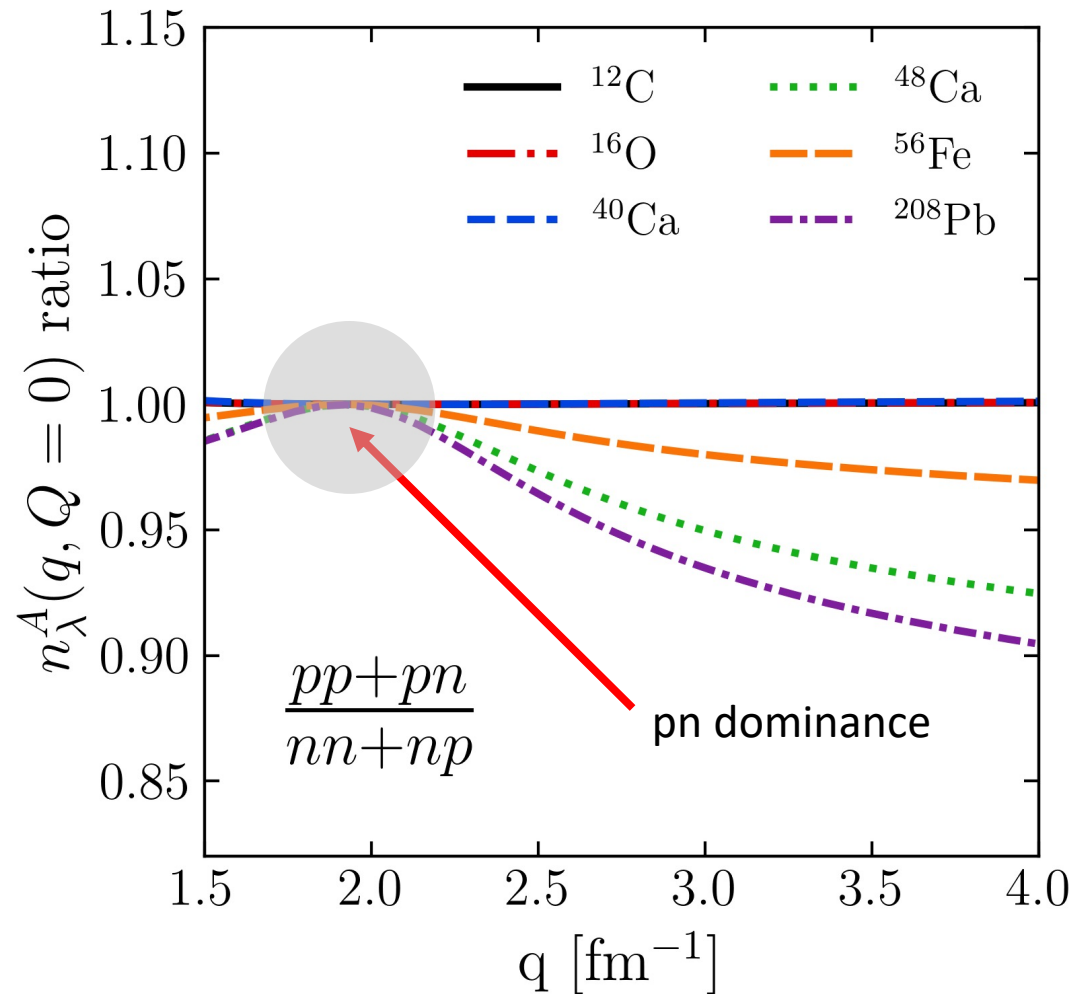pp/p scalar limit
N2LO
AV18

Relative Momentum [MeV/c]

• Reproduces the characteristics of cross section ratios using low RG resolution operator with simple approximations

Fig. 8: pp/pn ratio of pair momentum distributions under LDA with AV18 and $\lambda = 1.35$ fm^{-1}.

LDA results

- Ratio ~1 independent of N/Z in pn dominant region
- Ratio < 1 for nuclei where N > Z and outside pn dominant region

Fig. 9: (pp+pn)/(nn+np) ratio of pair momentum distributions under LDA with AV18 and $\lambda = 1.35$ fm^{-1}.

LDA results
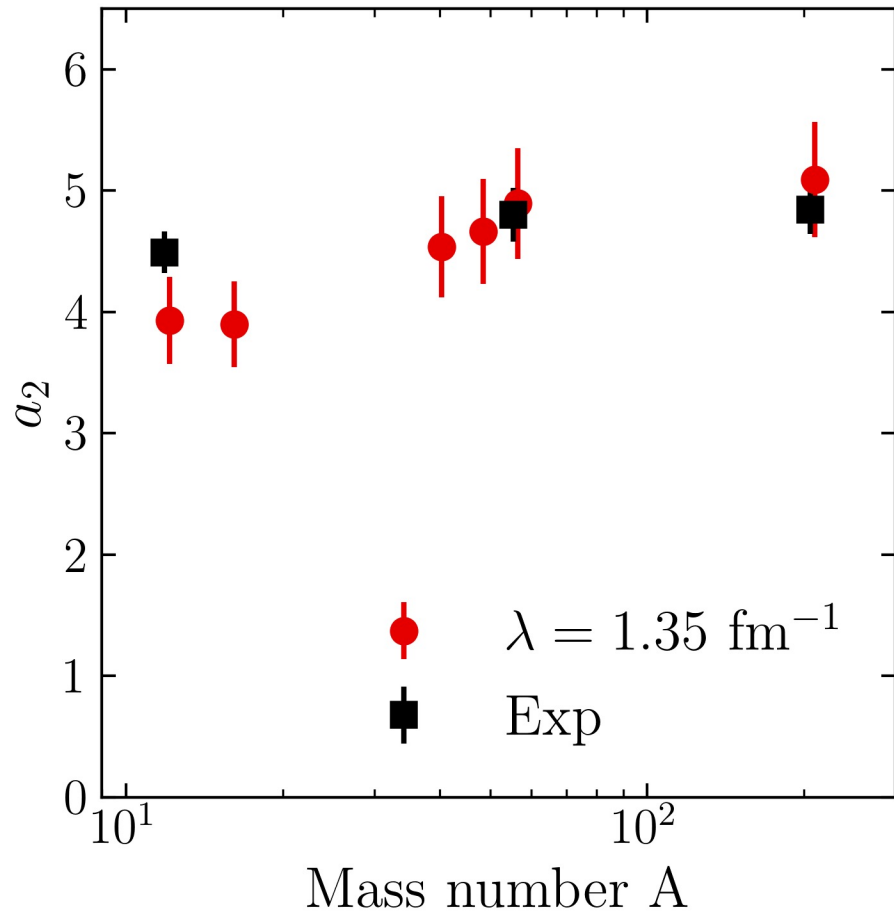

Fig. 10: a_2 scale factors using single-nucleon momentum distributions under LDA with AV18 and $\lambda = 1.35$ fm^{-1} compared to experimental values[1].

- SRC scale factors

$$a_2 = \lim_{q \to \infty} \frac{P^A(q)}{P^d(q)} \approx \frac{\int_{\Delta p^{high}} dq P^A(q)}{\int_{\Delta p^{high}} dq P^d(q)}$$

where $P^A(q)$ is the single-nucleon probability distribution in nucleus A with error bars from varying Δp^{high}

- Good agreement with a_2 values from experiment[1] and LCA calculations[2].

[1]B. Schmookler et al. (CLAS), Nature **566**, 354 (2019)
[2]J. Ryckebusch et al., Phys. Rev. C **100**, 054620 (2019)

Summary and outlook

- Simple approximations work and are systematically improvable at low RG resolution

- Results suggest that we can analyze high-energy nuclear reactions using low RG resolution structure (e.g., shell model) and consistently evolved operators
  - Matching resolution scale between structure and reactions is crucial!

- Ongoing work:
  - Extend to cross sections and test scale/scheme dependence of extracted properties
  - Further investigate how final state interactions and physical interpretations depend on the RG scale
  - Apply to more complicated knock-out reactions (SRG with optical potentials)
  - Implement uncertainty quantification

Extras

Similarity Renormalization Group (SRG)

- Evolve operators to low RG resolution

$$O(s) = U(s)O(0)U^{\dagger}(s)$$
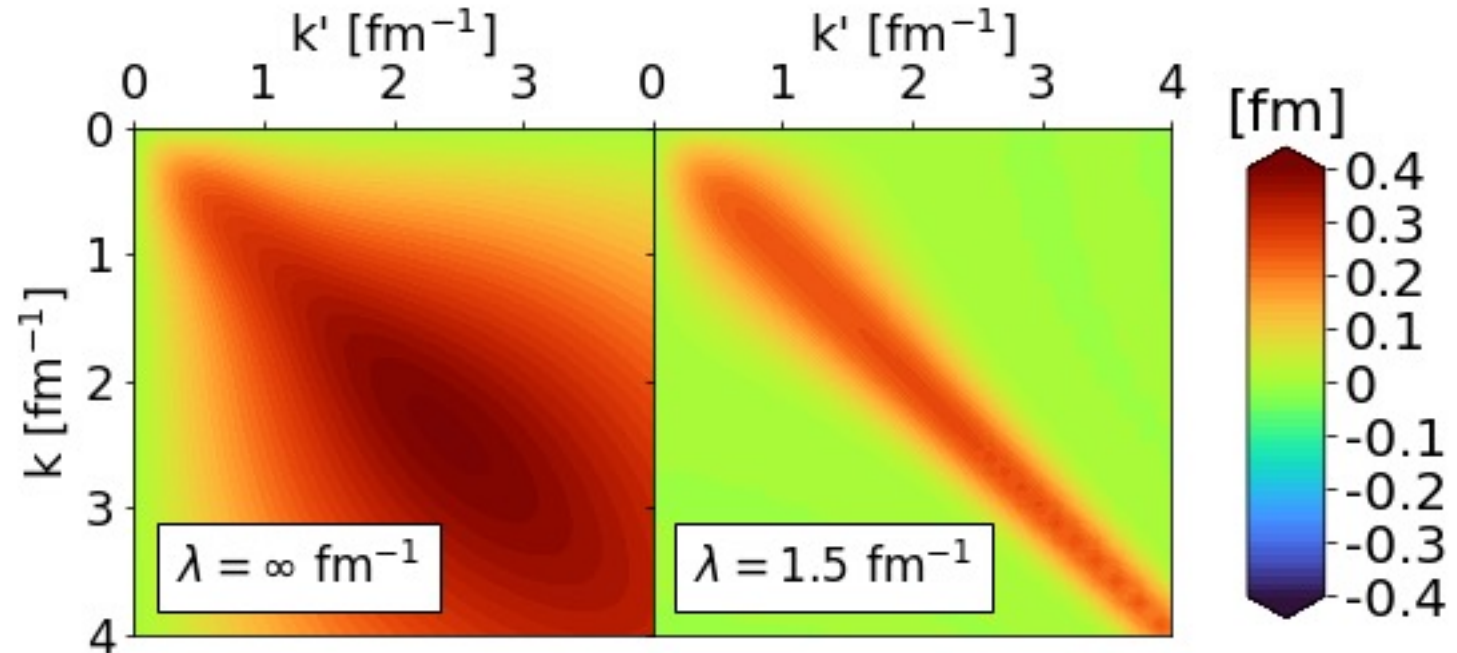
where $s = 0 \rightarrow \infty$ and $U(s)$ is unitary

Fig. 1: Momentum space matrix elements of Argonne v18 (AV18) under SRG evolution in $^1P_1$ channel.

Similarity Renormalization Group (SRG)

- Evolve operators to low RG resolution

$$O(s) = U(s)O(0)U^\dagger(s)$$

where $s = 0 \rightarrow \infty$ and $U(s)$ is unitary

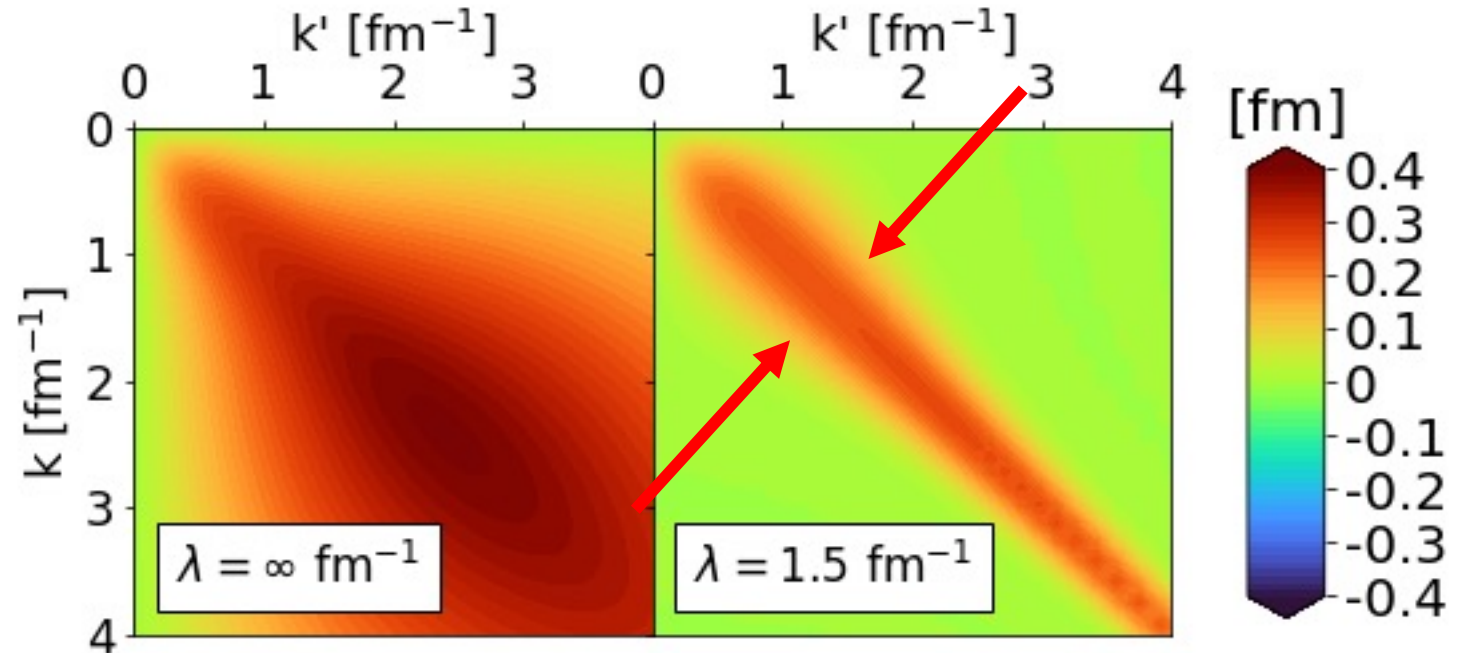- $\lambda = s^{-1/4}$ describes the decoupling scale of the RG evolved operator

Fig. 1: Momentum space matrix elements of Argonne v18 (AV18) under SRG evolution in $^1P_1$ channel.

Factorization